International Journal of Heat and Mass Transfer 93 (2016) 853–861

Contents lists available at ScienceDirect

International Journal of Heat and Mass Transfer

journal homepage: www.elsevier.com/locate/ijhmt

Radiative heat transfer from supersonic flow with suspended particles to a blunt body

Leonid A. Dombrovsky [a,*], Dmitry L. Reviznikov [b], Andrey V. Sposobin [b]

[a] Joint Institute for High Temperatures, Krasnokazarmennaya 17A, NCHMT, Moscow 111116, Russia
[b] Moscow Aviation Institute (Aerospace University), Volokolamskoe Shosse 4, Moscow 125993, Russia

ARTICLE INFO

Article history:
Received 1 September 2015
Received in revised form 4 October 2015
Accepted 26 October 2015

Keywords:
Radiative heat transfer
Supersonic flow
Blunt body
Absorbing and scattering particles
Collisions of particles
Computational model

ABSTRACT

The spectral radiative transfer problem for a supersonic gas flow with suspended particles at the front surface of a blunt body is solved using the combined two-step model based on transport approximation for the scattering phase function. The particle laden flow is calculated taking into account both dynamic and temperature non-equilibrium of micron-sized particles suspended in the carrier gas. A computational study of the problem showed that the effect of collisions between polydisperse particles including those reflected from the body is significant for both the flow field of particles behind the shock wave and the radiative heat transfer. At the same time, one can use a monodisperse approximation instead of complete calculations to estimate both the radiation flux and equilibrium temperature of the body surface.

1. Introduction

The problem of thermal interaction of a supersonic flow of a gas or plasma with a blunt body is very important in some aerospace applications. This interaction is especially strong in two cases: at very high relative velocities of the flow and also in the case when solid or liquid particles are suspended in a gas. The latter case is characterized by specific difficulties because of a complex behavior of composite materials under the action of a gas flow with particles [1]. The solid particles can increase essentially the heat transfer near the stagnation point. In the case of large particles impinging on the body surface, a contribution to the heat flux is related to transformation of the particle kinetic energy [2–4]. For fine particles, an increase in the heat flux is explained by modification of the flow in the boundary layer [5]. This problem of fluid mechanics has been theoretically studied in detail for wide ranges of particle sizes and free stream particle volume fraction in the recent paper [6].

It is well-known that a contribution of thermal radiation to combined heat transfer in supersonic flow over the bodies may be significant. This problem is usually considered as applied to the re-entry stage of space missions [7,8]. Most recent studies are focused on plasma radiation at very high re-entry velocity [9–13]. The presence of micron-sized particles makes this problem rather different from that for gas or plasma flow without particles. On the one hand, the complex radiative properties of the host medium appears to be not so important and there is no need in extremely detailed spectral calculations because of a continuous emission spectrum of particles. On the other hand, one should take into account both the local dynamic and thermal nonequilibrium of particles [1,6,14–18] and the radiation scattering by particles of size comparable with the wavelength [19–24].

The computational modeling of supersonic flows of a gas with suspended particles is not a simple task, especially in the case when collisions of particles with each other and also with the body surface are important. The flow model appears to be especially complex in the realistic case of a wide size distribution of particles because of numerous collisions between the particles of different size. In papers [23,24], the monodisperse approximation has been used. Of course, this approach simplified radically the mathematics of both the flow field and the radiative transfer calculations. At the same time, it was not clear how to choose an appropriate average size of particles in this approach and to estimate the errors of the monodisperse approximation in the main parameters of the calculated flow field and radiative transfer. Moreover, it is not obvious that this approach is applicable to the problem under consideration. In addition, one should recall the real cases when monodisperse approximation gives too crude results even for integral (over the spectrum) radiative flux from an isothermal particle

* Corresponding author. Tel.: +7 910 408 0186; fax: +7 495 362 5590.
E-mail address: ldombr@yandex.ru (L.A. Dombrovsky).

http://dx.doi.org/10.1016/j.ijheatmasstransfer.2015.10.072
0017-9310/

Nomenclature

a	particle radius
A, B	size-distribution parameters
$\vec{C}, \vec{F}, \vec{G}, \vec{N}, \vec{q}$	vectors in Eq. (6a)
D	radiation diffusion coefficient
E	internal energy
E_a, E_s	specific coefficients introduced by Eq. (22)
f_v	volume fraction of particles
$\vec{f}$	force
F	gamma-distribution
G	spectral incident radiation
H	enthalpy
I	radiation intensity
K	coefficient in Eq. (13)
l	the number of particle fractions
m	complex index of refraction or mass of particle
N_p	number of particles
q	radiative flux
Q	efficiency factor of absorption or scattering
R	radius of spherical body
s	coordinate along the body surface
S	emission term of the source function
x	diffraction parameter

Greek symbols

α	absorption coefficient
β	extinction coefficient
γ	specific heat ratio
ϵ	emissivity
κ	index of absorption
λ	wavelength
σ	scattering coefficient
σ_0	Stefan–Boltzmann constant
$\vec{\omega}$	angular velocity
$\vec{\Omega}$	unit vector of direction

Subscripts and superscripts

a	absorbed
b	blackbody
d	drag
m	maximum
M	Magnus
p	particle
r	radiative
s	scattered
t	total (integral)
tr	transport
w	wall
ω	rotational

cloud [19,22,25]. Note that this approximation is totally inapplicable for thermal radiation of some polydisperse systems when particles of different size have considerably different temperatures. The known examples are: thermal radiation of particles in plasma spraying [26–28], radiation from combustion products in exhaust plumes of aluminized-propellant rocket engines [19,21,22,29,30] and radiative cooling of core melt droplets in nuclear fuel–coolant interaction [31–33].

The objective of the present paper is twofold: (1) To summarize the methodological results for radiative transfer calculations presented in [24] for the case of numerous collisions between polydisperse particles [34] and (2) To examine the monodisperse approximation in the realistic case of equilibrium temperature of the body surface.

According to [34], the value of an average particle radius which gives good estimate of the radiative flux is different for relatively cold and hot surface of the blunt body. Therefore, the solution to the second task is not obvious. Note that possible use of the monodisperse approach is very promising to decrease the computational time. The latter is especially important for the conjugated problems with destruction of the body material under the combined thermal and mechanical action of the flow containing particles [1,18,35].

The results of recent analysis of different approximate methods in radiative transfer calculations reported by Dombrovsky and Reviznikov [24] are used in the present paper. According to these results, the traditional P_1 approximation is sufficiently accurate only in the case of a relatively cold body surface (see also papers [22,36–38]), whereas the combined method including the ray-tracing procedure [22,39] can be employed to solve the radiative transfer equation at the second step of numerical solution in the case of arbitrary temperature of the body surface.

The present study is motivated mainly by the interest to thermal conditions in the experimental testing of composite materials used in design of rocket engines. Therefore, we consider a model problem with parameters typical of engineering problems of this type. At the same time, the methods suggested are expected to be also applicable to some re-entry problems.

The present paper is focused mainly on elaboration of the advanced computational model and illustration of this model quality in the most important range of the problem parameters. Some specific features of the problem solution at various geometrical and thermal parameters have been already studied in recent publications by the authors [23,24,34].

2. Flow field model for gas with suspended particles

A general scheme of the problem under consideration is illustrated in Fig. 1 taken from recent paper [24]. The uniform supersonic flow of combustion products containing small alumina particles interacts with a blunt body. It is assumed that there are both dynamic and thermal equilibrium between the gas and small alumina particles in the exit cross section of the nozzle. In contrast to papers [23,24], the only variant of the geometrical parameters of the nozzle and spherical obstacle is considered: the radius 3 cm of the sphere, the radius 4.66 cm of the nozzle exit cross section and the distance 5.33 cm from the nozzle exit to the sphere center. This limitation is explained by the limiting length of the journal paper. The physical parameters of the model problem under consideration are similar to those reported in the above referred papers. At the nozzle exit, the specific heat ratio $\gamma = 1.25$, density $\rho = 0.6$ kg m^{-3}, pressure $p = 0.269$ MPa, temperature $T = 1558$ K, and Mach number M = 2 were taken. Note that the stagnation temperature is equal to $T_0 = 2336$ K at the above conditions. The initial volume fraction of particles is equal to $f_{v0} = 10^{-4}$. It was assumed that all particles, which reach the body surface, undergo specular reflection with the recovery factor equal to 0.9.

It is typical for the combustion problems that small volume elements contain a large number of particles, so that a representative local size distribution of particles can be introduced. For simplicity,

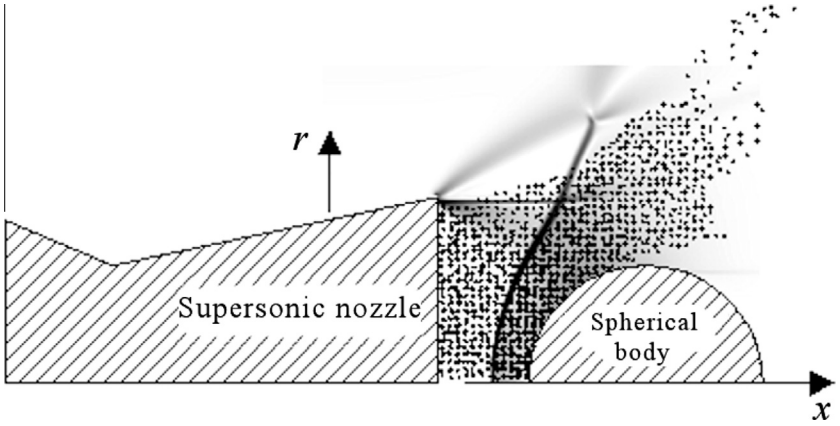

Fig. 1. Scheme of the problem and a part of the computational region.

we assume that all particles are spherical. In this case, the number of particles with radii in the range from a to $a + da$ in a unit volume is expressed as $N_p F(a)da$, where N_p is the total number of particles in this volume, $F(a)$ is the size distribution function. The above introduced function is normalized as follows:

$$\int_0^\infty F(a)da = 1 \tag{1}$$

It is convenient to introduce the volume fraction of particles:

$$f_v = \frac{4\pi}{3} N_p \int_0^\infty a^3 F(a)da \tag{2}$$

It is assumed also that size distribution at the initial cross section of the undisturbed flow is given by the following two-parameter gamma-distribution widely employed for disperse composition of natural and industrial aerosols [19–22,40–42]:

$$F(a) = \frac{A^{B+1}}{\Gamma(B+1)} a^B \exp(-Aa) \tag{3}$$

This distribution has a maximum at $a = a_m = B/A$, and the average particle radii can be easily calculated:

$$a_{i,i-1} = (B+i)/A = a_m + i/a \tag{4}$$

where the ordinary notation for the integral parameters of the particle size distribution is used:

$$a_{ij} = \int_0^\infty a^i F(a)da \Big/ \int_0^\infty a^j F(a)da \tag{5}$$

The typical curves of $F(a)$ are shown in Fig. 2.

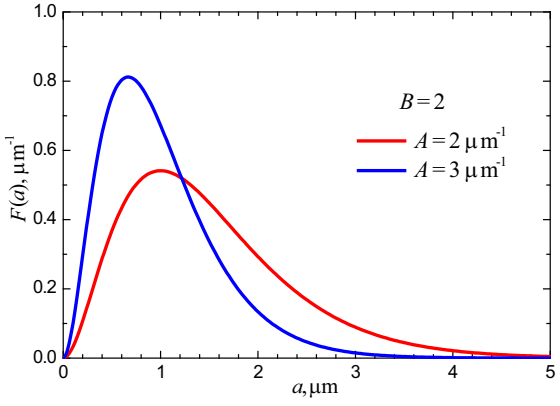

Fig. 2. Gamma-distributions of particle sizes.

The detached shock wave in front of the body leads to significant changes of the flow parameters and significant dynamical and thermal non-equilibrium between the micron-sized particles and the carrier gas flow. Of course, the local size distributions of particles are not the same as that in the initial cross section of the flow. The particles are heated behind the shock wave and their local volume fraction increases significantly as compared with that in the free flow. This leads to specific conditions of radiative transfer in this region. As to gases, we assume that both absorption and emission of the infrared radiation by gases can be neglected. This specific simplification is really acceptable because of a predominant role of condensed phase particles in all the thermal radiation effects in similar problems [19,22,43]. The spectral approach employed to calculate the complete radiation field and also the radiative flux at the body surface are presented in the next section of the paper.

The mathematical model of polydisperse flow is based on a combination of the Eulerian approach for the gas flow and the Lagrangian formulation for the velocity and temperature of suspended particles. The coupled equations for the gas flow take into account the effect of particles:

$$\frac{\partial \vec{q}}{\partial t} + \frac{\partial \vec{F}(\vec{q})}{\partial x} + \frac{\partial \vec{G}(\vec{q})}{\partial y} + \vec{C}(\vec{q}) = \vec{N} \tag{6a}$$

$$\vec{q} = \begin{pmatrix} \rho \\ \rho u \\ \rho v \\ \rho E \end{pmatrix} \vec{F} = \begin{pmatrix} \rho u \\ \rho u^2 + p \\ \rho uv \\ \rho uH \end{pmatrix} \vec{C} = \frac{\rho v}{y} \begin{pmatrix} 1 \\ u \\ v \\ H \end{pmatrix} \vec{G} = \begin{pmatrix} \rho v \\ \rho uv \\ \rho v^2 + p \\ \rho vH \end{pmatrix}$$

$$\vec{N} = \begin{pmatrix} 0 \\ -\langle f_{px} \rangle \\ -\langle f_{py} \rangle \\ -\langle \vec{f}_p \vec{v}_p + \vec{\tau}_\omega \vec{\omega}_p + q_c \rangle \end{pmatrix} \tag{6b}$$

$$E = \frac{p}{\rho(\gamma - 1)} + \frac{1}{2}(u^2 + v^2) \quad H = E + \frac{p}{\rho} \tag{6c}$$

where the components of vector $\vec{N}$ are the impulse and energy fluxes from particles to ambient gas. The nonlinear Eqs. (6a)–(6c) are solved numerically using the TVD-modified Harten–Lax–Van Leer scheme of the second order [44]. The approach of non-reflecting perfectly absorbing boundary conditions [45] is used to avoid a non-physical effect of wave reflection at the boundaries of computational region. The rectangular grid adapted to both the body surface and the flow pattern is used in numerical solution.

Boundary conditions at the curvilinear boundary are approximated according to the ghost-cell immersed method. The details of the computational procedure can be found in paper [18]. Note that effect of particles on the carrying gas flow is rather weak excluding a thin layer at the body surface.

The model of the particle motion takes into account collisions between particles and their reflection from the body surface. The Saffman lift force [46] which is considerable for relatively slow shear flows including the boundary layer in the vicinity of stagnation point [47,48] is not taken into account. A method of direct numerical simulation of the complex particle dynamics taking into account the collisions of polydisperse particles has been developed in papers [49,50]. The particles are modeled as rigid uniform spheres. The motion of a single particle in a gas flow is governed by the following equations:

$$m_{\mathrm{p}}\frac{d\vec{v}_{\mathrm{p}}}{dt}=\vec{f}_{\mathrm{p}}\quad J_{\mathrm{p}}\frac{d\vec{\omega}_{\mathrm{p}}}{dt}=\vec{\tau}_{\omega} \tag{7}$$

The external force $\vec{f}_{\mathrm{p}}$ is a sum of the drag force $\vec{f}_{\mathrm{d}}$ and Magnus force $\vec{f}_{\mathrm{M}}$ responsible for the particle rotation:

$$\vec{f}_{\mathrm{p}}=\vec{f}_{\mathrm{d}}+\vec{f}_{\mathrm{M}} \tag{8a}$$

$$\vec{f}_{\mathrm{d}}=\frac{\pi a^2}{2}c_{\mathrm{d}}\rho(\vec{v}-\vec{v}_{\mathrm{p}})|\vec{v}-\vec{v}_{\mathrm{p}}|$$
$$\vec{f}_{\mathrm{M}}=\pi a^3 c_{\omega}\rho\left[\left(\frac{1}{2}\nabla\times\vec{v}-\vec{\omega}_{\mathrm{p}}\right)\times(\vec{v}-\vec{v}_{\mathrm{p}})\right] \tag{8b}$$

The drag coefficient is a function of Mach and Reynolds numbers. The dependence of $c_{\mathrm{d}}=c_{\mathrm{d}}(\mathrm{Re}_{\mathrm{p}},\mathrm{M}_{\mathrm{p}})$ is calculated using the formula by Henderson [51]. The torque value is determined as follows:

$$\vec{\tau}_{\omega}=\frac{a^5}{2}c_{\mathrm{l}}\rho\left(\frac{1}{2}\nabla\times\vec{v}-\vec{\omega}_{\mathrm{p}}\right)\left|\frac{1}{2}\nabla\times\vec{\tau}-\vec{\omega}_{\mathrm{p}}\right| \tag{8c}$$

The expressions for coefficients $c_{\omega}=c_{\omega}(\mathrm{Re}_{\mathrm{p}},\mathrm{Re}_{\omega})$ and $c_l=c_l(\mathrm{Re}_{\omega})$ can be found in papers [52–54].

Strictly speaking, the energy equation for particles should include a term corresponding to the contribution of thermal radiation. The radiative component of the total heat flux to moving particles can be determined from the radiation field as discussed in [22]. Theoretical estimates showed that particle temperature in the problem under consideration is determined by convective heat transfer with ambient gas and the role of thermal radiation can be neglected [24]. As a result, the energy equation for single particles is as follows:

$$c_{\mathrm{p}}m_{\mathrm{p}}\frac{dT_{\mathrm{p}}}{dt}=q_{\mathrm{c}}\quad q_{\mathrm{c}}=2\mathrm{Nu}\pi ak(T_0-T_{\mathrm{p}}) \tag{9}$$

where c_{p} is the heat capacity of particle material, q_{c} is the convective heat flux, k is the thermal conductivity of ambient gas, T_{p} is the particle temperature. The value of T_0 is assumed to be approximately equal to the stagnation temperature

$$T_0=T+|\vec{v}-\vec{v}_{\mathrm{p}}|^2/2c_{\mathrm{p}} \tag{10}$$

The Nusselt number Nu is calculated according to [55]. The coupled equations for particle motion and heat transfer are integrated using the fifth-order Runge–Kutta method. Of course, the equations for gas and those for particles are not independent ones. Therefore, these equations are solved simultaneously at each time of the general numerical procedure.

While modeling the flow with suspended polydisperse particles it is important to take into account numerous collisions between the particles. As a rule, the Monte Carlo methods similar to those applied in rarefied gas dynamics are used to simulate this effect [56,57]. According to [34], an alternative method of direct numerical simulation of particle dynamics suggested in [49] is employed in the present paper. According to this method, the particle motion during time interval $(t_{\mathrm{k}}, t_{\mathrm{k+1}})$ is computed using the analytical approximation of particle trajectory by second-order polynomials like the following one:

$$\vec{r}(t)=\vec{r}_2(t-t_{\mathrm{k}})^2+\vec{r}_1(t-t_{\mathrm{k}})+\vec{r}_0 \tag{11}$$

The condition of collision of two particles with radii a_i and a_j is given by the obvious forth-order algebraic equation:

$$|\vec{r}_i(t)-\vec{r}_j(t)|^2=(a_i+a_j)^2 \tag{12}$$

The dynamic parameters of a pair of particles after their collision and also the characteristics of a particle after reflection from the body surface are calculated on the basis of the model of hard spheres [17]. Successive treatment of all the collisions is carried out using unified queue of events sorted chronologically. Note that each particle can participate in multiple collisions with other particles and body surface during one computational step. Note that an assumption of a specular reflection in every collision of particles with the recovery factor equal to 0.9 was used in the calculations.

The above described approach enables one to calculate accurately the complex flow field taking into account the repeated collisions between the particles and their reflection from the body surface. At the same time, the implementation of this method to the computer code may lead to very time-consuming algorithm because of difficulties of parallel calculations. Some ways to minimize the computational time have been discussed in [57]. One of these ways is used in the present paper. We represent every K particles by a single probe particle. As a result, Eq. (12) is modified:

$$|\vec{r}_i(t)-\vec{r}_j(t)|^2=K(a_i+a_j)^2 \tag{13}$$

Note that the probe particle has physical properties of a single particle. But we should use the coefficient K to obtain some integral properties such as the effect of particles on the gas flow and the impact of particles on the body surface. Therefore, it is important to be sure that a probe particle has the same intensity of collisions along the trajectory as that of a single particle. The probe particles approach is expected to extend possible applications of the direct numerical simulation of particle collisions because of a significant decreasing both the computer memory and the computational time.

3. Radiative transfer modeling

In this paper, we do not consider the region past a body where there are no condensed phase particles. This makes possible to use the well-known P_1 approximation [22,58,59] at least at the first step of solution when the incident radiation field is determined. This approach leads to the boundary-value problem for the modified Helmholtz equation:

$$-\nabla(D\nabla G)+\alpha G=4\pi S\quad D=1/(3\beta_{\mathrm{tr}})\quad S=\sum_{i=1}^{l}\alpha_i I_{\mathrm{b}}(T_{\mathrm{p,i}})\quad \alpha=\sum_{i=1}^{l}\alpha_i \tag{14}$$

where D is the spectral radiation diffusion coefficient, $\beta_{\mathrm{tr}}=\alpha+\sigma_{\mathrm{s}}^{\mathrm{tr}}$ is the transport extinction coefficient, $\sigma_{\mathrm{s}}^{\mathrm{tr}}=\sum_{i=1}^{l}\sigma_{\mathrm{s,i}}^{\mathrm{tr}}$ is the transport scattering coefficient, i is the current number of the particle fraction with temperature $T_{\mathrm{p,i}}$, l is the total number of particle fractions in the elementary volume. Of course, the spectral incident radiation G, the temperatures $T_{\mathrm{p,i}}$, and all coefficients in Eq. (14) are the functions of spatial coordinate $\vec{r}$. Hereafter, the subscript λ, which is usually used for spectral values, is omitted for brevity. Note that $S=\alpha I_{\mathrm{b}}(T_{\mathrm{p}})$ in the case when all particles have

the same temperature $T_p(\vec{r})$. However, this is not the case even for particles of the same size because of reflection of particles from the body surface.

It should be noted that a contribution of absorbing and emitting components of the carrying gas to radiative heat transfer in the problem under consideration is small and can be neglected. This is a typical situation for combustion products of aluminized propellants in solid-propellant rocket engines [19–22].

The Marshak boundary condition for Eq. (14) at the body surface with temperature T_w and spectral emissivity ε_w is as follows [22]:

$$-D(\vec{n}\nabla G) = \frac{\varepsilon_w}{2(2-\varepsilon_w)}(G - 4\pi I_b(T_w)) \tag{15}$$

where $\vec{n}$ is the external normal to the body surface. Obviously, the boundary conditions at other surfaces of the computational region are much simpler than that given by Eq. (15). With the use of the P_1 solution, the local spectral and integral radiative fluxes to the body surface are determined as follows:

$$q_w = \frac{\varepsilon_w}{2(2-\varepsilon_w)}(G - 4\pi I_b(T_w)) \quad q_w^t(s) = \int_{\lambda_1}^{\lambda_2} q_w(s)d\lambda \tag{16}$$

where s is the current curvilinear coordinate along the body surface. Of course, the spectral interval (λ_1, λ_2) should include the range of a considerable spectral contribution to the integral radiative flux.

The P_1 approximation is simple and very convenient for radiative transfer calculations especially in combined heat transfer problems. Moreover, this approach appears to be sufficiently accurate in the case when one needs only the divergence of radiative flux in the energy equation [60–62]. At the same time, the use of P_1 in radiative flux calculations at the boundaries of the computational region may lead to significant errors. A physical analysis of these errors has been studied in early paper by Dombrovsky [36] (see monograph [22] for more details). Nevertheless, the simplicity of this approach is a permanent reason of its use even in calculations of the radiation field around blunt-body vehicles in the atmosphere [37,38,63].

It is important that P_1 approximation can be derived from the complete radiative transfer equation by using the only assumption on the following linear angular dependence of the spectral radiation intensity:

$$I(\vec{r}, \vec{\Omega}) = \frac{1}{4\pi}[G(\vec{r}) + 3\vec{\Omega}\cdot\vec{q}(\vec{r})] \tag{17}$$

Generally, the P_1 is thought to be applicable in optically thick media. This widespread error is easily overcome if we recall that that this approach gives rather accurate results for 1-D problems of self emission of isothermal volumes of a homogeneous media at arbitrary optical thickness (see [22] for more details). In fact, the only condition of a sufficiently smooth angular structure of the radiation field, Eq. (17), is a basis of the P_1 applicability. This statement will be used in our analysis of the computational data obtained for the problem under consideration.

Radiative transfer is often characterized by complex angular dependences of the radiation intensity. In this case, the diffusion approximation can be incapable of accurately predicting the radiation field in real applications, especially for media that are characterized by strong spatial variation of radiative properties and large temperature gradients [36]. At the same time, even for the most complicated cases, the field of the radiation energy density (or incident radiation) obtained by using the diffusion approximation can be successfully used as an initial guess in multi-step solution methods [39,64].

Following this general idea suggested originally by Edwards and Bobcôo [65] (see also [22,64]), a next step in radiative transfer modeling was made in [24] as compared with [23]. No changes in energy equations for particles should be made. The only novelty is in additional iterative step in calculations of spectral radiative flux at the body surface. This enables us to estimate an error of the P_1 approximation. It is important (and very convenient) that this iteration can be made after completing the calculations because our current approach does not contain any feedback depending on the radiative heat flux at the body surface.

In transport approximation for the scattering phase function [64], the radiative transfer equation can be written as follows:

$$\vec{\Omega}\nabla I + \beta_{tr} I = \frac{\sigma_s^{tr}}{4\pi} G + S \quad G = \int_{(4\pi)} I d\vec{\Omega} \tag{18}$$

Eq. (18) with the variable incident radiation $G(\vec{r})$ determined using P_1 approximation at the first step of the combined two-step solution is integrated numerically along the rays (first toward the body surface and then in the opposite direction). A set of $61 \times 61 = 3721$ rays coming to the selected point of the body surface are used in this procedure. Up to one thousand of uniform intervals are used in the numerical integration along each ray. The boundary condition of perfect reflection and the alternative condition of zero spectral radiation intensity are considered at the external boundary of the computational region, but the difference between the results obtained with the use of these boundary conditions appeared to be negligible. Note that the second variant of the external boundary condition gives an upper estimate of the radiative flux at the body surface in the case of a relatively hot body. The boundary condition of both diffuse reflection and emission of radiation at the body surface is used in the calculations. It is assumed that the body material is opaque and the surface reflectivity is equal to $1 - \varepsilon_w$. For simplicity, the body surface is assumed to be gray (with optical properties independent of the wavelength). Having in mind the temperature level in the model problem, the wavelength range $0.5 \leqslant \lambda \leqslant 8.5$ μm was considered in the spectral radiative transfer calculations. It was shown that a uniform step of $\Delta\lambda = 0.1$ μm over the spectrum is quite sufficient for the reliable calculations of integral (over the spectrum) radiative flux at the body surface.

4. Radiative properties of particles

According to Mie theory [66,67], absorption and scattering properties of single spherical particles are controlled by two dimensionless parameters. The first one is the so-called diffraction or size parameter $x = 2\pi a/\lambda$ and the second one is the complex index of refraction of the particle substance $m = n - i\kappa$, where n is the index of refraction and κ is the index of absorption. The following approximations of spectral and temperature dependences for both indices of refraction and absorption of alumina are used in the calculations [22]:

$$n(\lambda, T) = n_0(\lambda)[1 + \varsigma_1(T - T_1)] \quad \varsigma_1 = 2.02\cdot 10^{-5} K^{-1} \quad T_1 = 473\,\mathrm{K} \tag{19a}$$

$$n_0^2 - 1 = \frac{1.024\lambda^2}{\lambda^2 - 0.003776} + \frac{1.058\lambda^2}{\lambda^2 - 0.01225} + \frac{5.281\lambda^2}{\lambda^2 - 321.4} \tag{19b}$$

$$\kappa(\lambda, T) = 0.002(1 + 0.7\lambda + 0.06\lambda^2)\,\exp[\varsigma_2(T - T_2)]$$
$$\varsigma_2 = 1.847\cdot 10^{-3}\mathrm{K}^{-1} \quad T_2 = 2950\ \mathrm{K} \tag{20}$$

Note that wavelength λ in Eqs. (19b) and (20) is expressed in microns. Eq. (20) has been originally suggested for molten alumina ($T > 2320$ K), but their use at lower temperatures gives an acceptable qualitative estimate for the index of absorption of solid substance. At least, it seems to be appropriate for the model problem under consideration.

The following approximate relations for particles of a weakly absorbing substance are used to calculate the efficiency factor of absorption Q_a and the transport efficiency factor of scattering Q_s^{tr} [22]:

$$Q_a = \frac{4n}{(n+1)^2}[1-\exp(-5\kappa x)] + 2.5\kappa\psi/e_1 \tag{21a}$$

$$Q_s^{tr} = \begin{cases} 1.2\psi[1-15(2.5-n)\kappa] \text{ when } \varphi \leqslant 8 \\ x^{-\xi} + 0.5\psi(1-10\kappa)(n-1)(2.5-n) \text{ when } \varphi > 8 \end{cases} \tag{21b}$$

where

$$\xi = 0.75 - 0.3n + (32.5-10n)\kappa \quad \psi = \varphi(n-1)e_1^2$$
$$e_1 = \exp(-0.1\varphi) \quad \varphi = 2x(n-1) \tag{21c}$$

Note that the use of approximations (21a)–(21c) is much preferable than time-consuming calculations based on the Mie theory. Typical results of calculations using these approximate equations for alumina particles with size distributions of Fig. 2 are presented in Fig. 3. The values of specific absorption coefficient and transport scattering coefficient defined as

$$E_a = \alpha/f_v \quad E_s^{tr} = \sigma_s^{tr}/f_v \tag{22}$$

are plotted together with the results obtained using the exact Mie theory. One can see in Fig. 3 that approximate spectral calculations of both the absorption coefficient and transport scattering coefficient are sufficiently accurate to be used in the present study and there is no need in time-consuming Mie theory calculations. It should be noted that absorption is relatively small over the spectrum and $Q_s^{tr} \gg Q_a$ even at temperature of alumina particles equal to T_p = 2300 K. Both the predominant role of scattering and insignificant effect of size distribution on absorption are important for understanding the results of subsequent radiative transfer calculations.

The local volume fraction of alumina particles is not so great to take into account the so-called dependent scattering. The latter statement is not absolutely correct because of significant increase of the volume fraction of small particles near the body surface. Nevertheless, our approach is based on the widely used hypothesis of independent scattering [68–70]. It means that each particle is assumed to absorb and scatter the radiation in exactly the same manner as if other particles did not exist. In addition, there is no systematic phase relation between partial waves scattered by individual particles during the observation time interval, so that the intensities of the partial waves can be added without regard to phase. In other words, each particle is in the far-field zones of all other particles, and scattering by individual particles is incoherent.

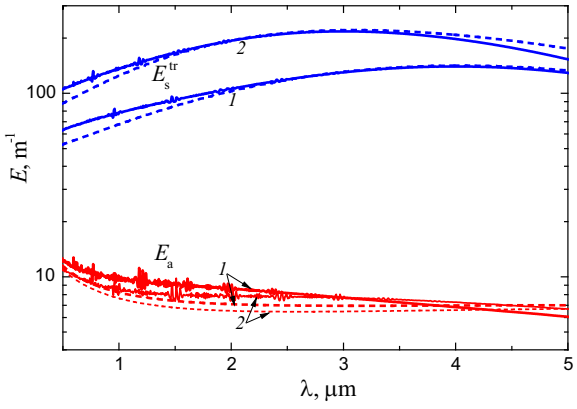

Fig. 3. Specific absorption coefficient and transport scattering coefficient of polydisperse alumina particles with size distribution (3) at B = 2 and A = 2 μm^{-1} (*1*) and A = 3 μm^{-1} (*2*) at T_p = 2300 K: solid lines – calculations using the Mie theory, dashed lines – calculations using Eqs. (21a)–(21c).

5. Analysis of numerical results

First of all, the effect of collisions between particles on both the flow field and radiative transfer is analyzed. The minimum estimate of this effect can be done on the basis of the monodisperse approach. In this case, the most of collisions between particles are localized in the compressed medium layer behind the shock wave. An expected qualitative result on the role of collisions between alumina particles behind the shock wave is illustrated in Fig. 4. A detailed mesh was used in the flow field calculations. It was shown that transfer from the mesh 600 × 900 to 1200 × 1800 has little impact on computational results. As usually, the steady-state solution was obtained using the convergence of a transient solution after about 10^3–10^4 time steps. The total number of particles considered at every time step of duration 10^{-7} s was about $3\cdot10^6$ with more than 10^5 collisions between them and about 10^3 collisions of particles with the body surface.

The changes of both the volume fraction of particles and their temperature (hot particles are shown in red) are obvious from comparison of the left and right-hand panels in this figure. There is a sharp boundary of the region of hot particles in calculations without taking into account collisions between particles (left panel). It is explained by the predominant contribution of particles reflected from the body surface. The collisions between the main stream particles and reflected particles lead to much narrower layer of hot particles. This layer appeared to be significantly closer to the body surface. This effect is known from previous computational studies [14,16,18] but the radiative transfer was not considered in these papers.

It is interesting that collisions between alumina particles lead also to some changes in the current particle size distribution. This statement is illustrated in Fig. 5, where some numerical data on size distribution of particles at the body surface are presented. In the region near the stagnation point, the collisions between particles lead to a bit wider size distribution (Fig. 5a). At the same time, the effect of collisions between "primary" and reflected particles on the overall size distribution increases with the distance along the body surface and appears to be very strong in the region far from the stagnation point (Fig. 5b). In calculations without collisions one can distinguish separate size distributions of small primary particles and large reflected ones. The collisions lead to a significant transformation of this bimodal distribution with a great decrease in the relative volume fraction of alumina particles which have the radius greater than about 1.7 μm. As one can expect, the effect of flow field changes shown in Figs. 4 and 5 on the integral (over the spectrum) radiative flux at the front surface of a body is significant, at least in the case of a relatively cold body surface considered in paper [34]. These results are reproduced in Fig. 6 where the relative value of $\bar{q}_w^t = q_w^t/(\sigma_0 T_0^4)$ is plotted as a function of the dimensionless coordinate along the body surface $\bar{s} = s/R$ (s is measured from the stagnation point). One can see that collisions between particles lead to significant increase in the radiative flux even in the case of monodisperse alumina particles. It is a clear illustration of the great role of collisions between alumina particles in radiative transfer calculations. Note that simplified approach based on P_1 approximation only was used in these calculations because this approach is acceptable in the case of a cold body surface [24]. The computational procedure based on P_1 approximation can be easily employed using a detailed mesh without considerable increase in the time of complete calculations.

It is interesting to examine an applicability of the monodisperse approximation to approximate calculations of the integral

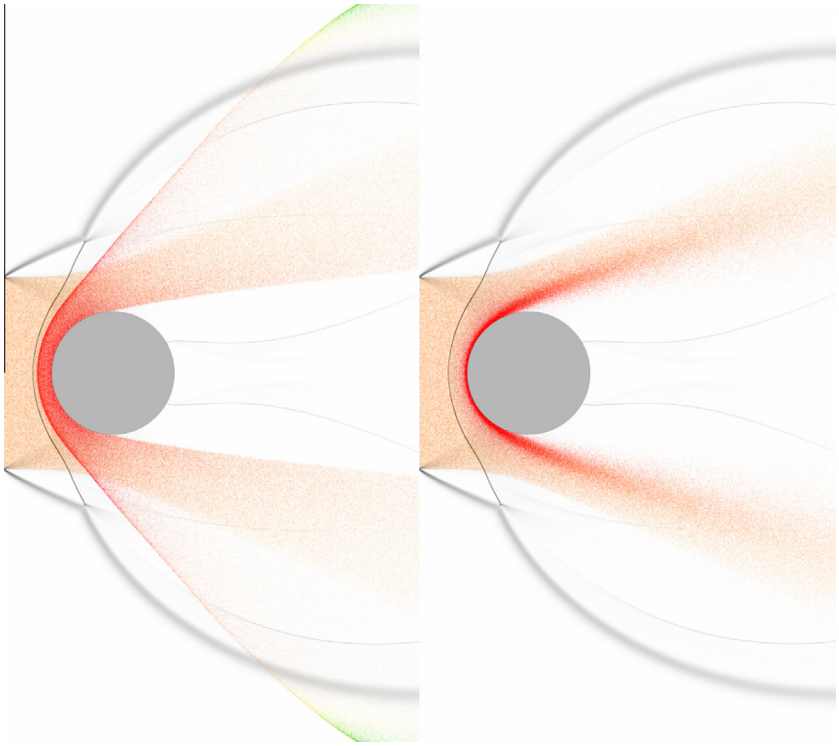

Fig. 4. Temperature fields of monodisperse alumina particles with radius $a = 2.5$ μm: left panel – calculations without effects of collisions between particles, right panel – complete calculations. Results of two-phase flow field calculations.

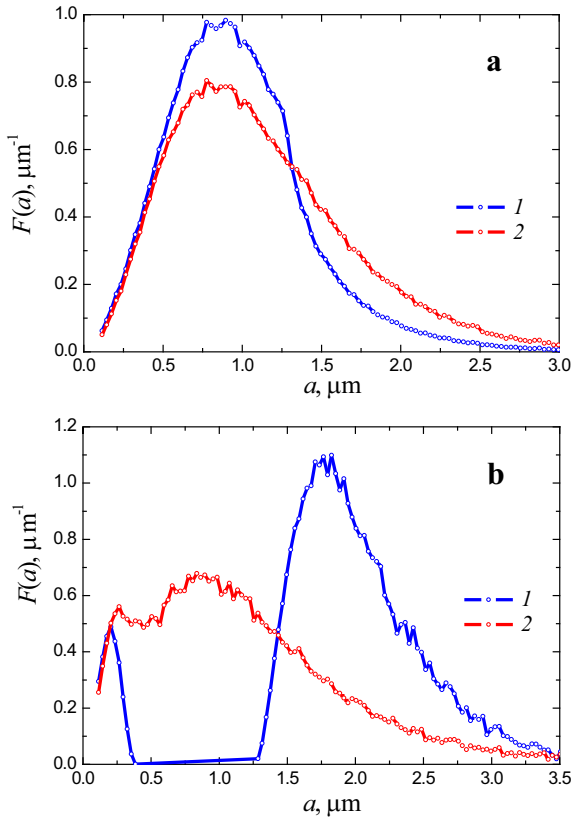

Fig. 5. Size distribution of alumina particles (a) near the stagnation point at the body surface and (b) rather far (at angles 80–90°) from the stagnation point in the case of initial gamma-distribution with parameters $B = 2$ and $A = 3$ μm^{-1}: *1* – calculations without collisions between particles, *2* – complete calculations. Results of calculations based on P_1 approximation.

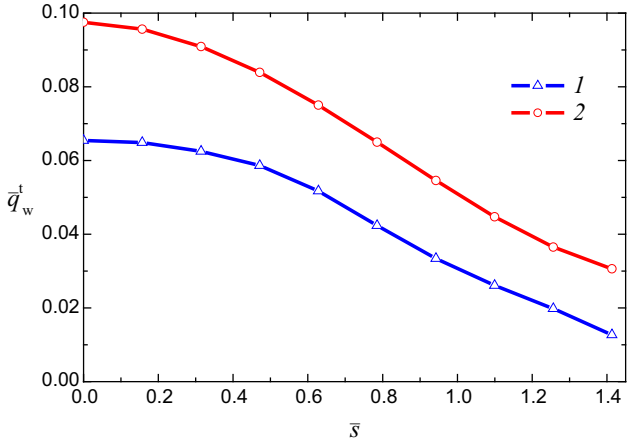

Fig. 6. Profiles of the relative radiative flux along the body surface at $a = 2.5$ μm: *1* – calculations without collisions between particles, *2* – complete calculations.

radiative flux. The result obtained recently by the authors [34] is very promising: one can really calculate the radiative flux at the front surface of the blunt body and the error of these approximate calculations is insignificant. It is sufficient to use different average radii of alumina particles for two opposite cases of a cold or very hot surface of the body. These average radii are equal to a_{43} and a_{32} in the cases of a cold and hot surface of the body, respectively.

Note that monodisperse approximation does not lead to a significant decrease in computational time with the use of the above described general procedure of detailed calculations. At the same time, the monodisperse approach is expected to be very useful because it can be employed in a combination with simpler flow models when the calculations are not so time-consuming. As to the radiation calculations, the difference in the computational time between the polydisperse and monodisperse variants is

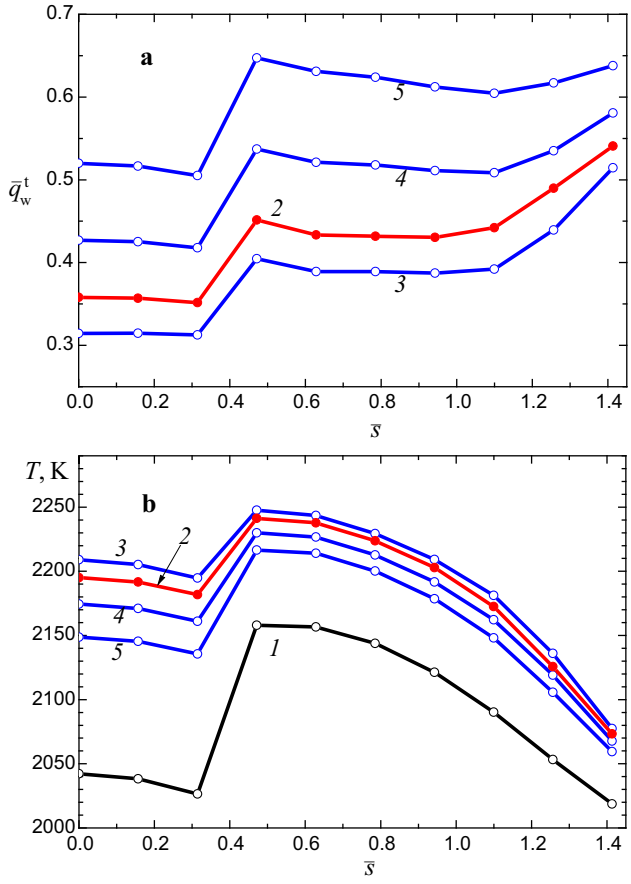

Fig. 7. Calculated profiles of (a) total radiative flux and (b) a conventional equilibrium temperature along the body surface: *1* – flow without suspended particles, *2* – polydisperse alumina particles at $A = 3\ \mu m^{-1}$ and $B = 2$, *3–5* – monodisperse particles with radii $a = 1.5\ \mu m$, 2 μm, and 2.5 μm, respectively.

insignificant because approximate relations are used for spectral radiative properties of alumina particles instead of Mie calculations.

Let us consider more realistic case of a quasi-steady regime of the body heating. For simplicity, it is assumed that the local "equilibrium" temperature of the body surface is determined by a balance between convective and radiative heat fluxes. In other words, both heat transfer by conduction in the body and possible destruction of the body material are not taken into account. The calculated profiles of the integral radiative flux and the resulting temperature of the body surface are presented in Fig. 7. Note that non-monotonic behavior of these profiles is explained by a transition from the laminar to turbulent flow regime. It is important that the contribution of thermal radiation to the equilibrium temperature of the body surface is significant and this effect can be well described using the monodisperse approximation for polydisperse alumina particles with equivalent average radius $a_{32} = 1.67\ \mu m$.

6. Conclusions

A general computational model for the supersonic flow with suspended polydisperse particles was developed. This model includes the flow field calculations in the case of a detached shock wave in front of a blunt body taking into account not only the dynamic and temperature nonequilibrium of particles but also numerous collisions of particles between each other and with the body surface. The spectral radiative transfer is an important part of this general model which enables one to obtain the radiative flux at the body surface. According to recent studies by the authors, the combined method including the P_1 approximation at the first step of an iterative solution and the ray-tracing procedure for subsequent integration of transport radiative transfer equation is implemented into the general code.

The numerical analysis showed that collisions between "primary" particles coming with the main gas flow and particles reflected from the body surface have a significant effect on both the motion of particles and the radiative transfer. Of course, the qualitative estimates obtained in the present paper depend on the body material structure which is responsible for the reflection character of alumina particles.

The calculations for polydisperse alumina particles with a typical size distribution showed that one can obtain reliable estimates of integral (over the spectrum) radiative flux at the front surface of a body on the basis of relatively simple monodisperse approximation. At the same time, the effective radius of monodisperse particles depends considerably on the problem parameters. In particular, one can use the Sauter average radius a_{32} in a realistic case of quasi-steady temperature of the body surface. Note that possible use of monodisperse model is especially important in engineering calculations to solve conjugated problems characterized by thermal or mechanical destruction of the body material when the detailed calculations for complex size distributions of suspended particles are too time-consuming.

The paper can be considered as a theoretical and computational basis of regular engineering calculations at various geometrical and physical parameters of the problem and also as a potential part of general computational models for conjugated problems of combined heat transfer.

Acknowledgements

The authors are grateful to the Russian Foundation for Basic Research for the financial support of this study under Grants No. 13-08-00022a and 15-08-06262a.

References

[1] D.S. Mikhatulin, Yu.V. Polezhaev, D.L. Reviznikov, Heat Transfer and Destruction of Bodies in a Supersonic Heterogeneous Flow, Yanus-K, Moscow, 2007 (in Russian).
[2] E.B. Vasilevsky, L.A. Dombrovsky, D.S. Mikhatulin, Yu.V. Polezhaev, Heat transfer in the neighborhood of the stagnation point under conditions of hypersonic heterogeneous slip flow past bodies, High Temp. 39 (6) (2001) 860–873.
[3] E.B. Vasilevsky, L.A. Dombrovsky, D.S. Mikhatulin, Yu.V. Polezhaev, Heat transfer in a heterogeneous supersonic flow, Heat Transfer 2002, in: Proc. of 12th Int. Heat Trans. Conf. (IHTC-12), 3, Grenoble, France, 2002, pp. 177–182.
[4] A.N. Osiptsov, L.A. Egorova, V.I. Sakharov, B. Wang, Heat transfer in supersonic dusty-gas flow past a blunt body with inertial particle deposition effect, Prog. Nat. Sci. 12 (12) (2002) 887–892.
[5] E.B. Vasilevsky, A.N. Osiptsov, A.V. Chirikhin, L.V. Yakovleva, Heat exchange on the front surface of a blunt body in a high-speed flow containing low-inertia particles, J. Eng. Phys. Thermophys. 74 (6) (2001) 1399–1411.
[6] B. Oesterlé, A.N. Volkov, Yu.M. Tsirkunov, Numerical investigation of two-phase flow structure and heat transfer in a supersonic dusty gas flow over a blunt body, in: Ph. Reijasse, D. Knight, M. Ivanov, I. Lipatov (Eds.), Progress in Flight Physics, vol. 5, EDP Sci., Les Ulis (France), 2013, pp. 441–456.
[7] S.T. Surzhikov, Radiative gas dynamics of large landing spacecraft, High Temp. 48 (6) (2010) 910–917.
[8] J.S. Shang, S.T. Surzhikov, Nonequilibrium radiative hypersonic flow simulation, Prog. Aerosp. Sci. 53 (2012) 46–65.
[9] J.-M. Lamet, P. Rivière, M.-Y. Perrin, A. Soufiani, Narrow-band model for nonequilibrium air plasma radiation, J. Quant. Spectrosc. Radiat. Transfer 111 (1) (2010) 87–104.
[10] A. Feldick, M.F. Modest, An improved wavelength selection scheme for Monte Carlo solvers applied to hypersonic plasmas, J. Quant. Spectrosc. Radiat. Transfer 112 (8) (2011) 1394–1401.
[11] A. Feldick, M.F. Modest, A spectrally accurate two-dimensional axisymmetric, tightly coupled photon Monte Carlo radiative transfer equation solver for hypersonic entry flows, ASME J. Heat Transfer 134 (12) (2012). Paper 122701.

[12] J.S. Shang, D.A. Andrienko, P.G. Huang, S.T. Surzhikov, A computational approach for hypersonic nonequilibrium radiation utilizing space partitions algorithm and Gauss quadrature, J. Comput. Phys. 266 (2014) 1–21.
[13] C.M. Mazzoni, D. Lentini, G. D'Ammando, R. Votta, Evaluation of radiative heat transfer for interplanetary re-entry under vibrational nonequlibrium conditions, Aerosp. Sci. Technol. 28 (1) (2013) 191–197.
[14] A.N. Volkov, Yu.M. Tsirkunov, Effect of a dispersed admixture on the flow pattern and heat transfer in a supersonic dusty-gas flow around a cylinder, Fluid Dyn. 40 (4) (2005) 561–574.
[15] A.N. Volkov, Yu.M. Tsirkunov, B. Oesterlé, Numerical simulation of a supersonic gas–solid flow over a blunt body: the role of inter-particle collisions and two-way coupling effects, Int. J. Multiphase Flow 31 (12) (2005) 1244–1275.
[16] V.V. Vinnikov, D.L. Reviznikov, A.V. Sposobin, Two-phase shock layer in a supersonic dusty gas flow, Math. Models Comput. Simul. 2 (4) (2010) 514–525.
[17] C.T. Crowe, J.D. Schwarzkopf, M. Sommerfeld, Y. Tsuji, Multiphase Flows with Droplets and Particles, second ed., CRC Press, New York, 2011.
[18] T.V. Ershova, D.S. Mikhatulin, D.L. Reviznikov, A.V. Sposobin, V.V. Vinnikov, Numerical simulation of heat and mass transfer between heterogeneous flow and an obstacle, Comput. Therm. Sci. 3 (1) (2011) 15–30.
[19] L.A. Dombrovsky, Radiation Heat Transfer in Disperse Systems, Begell House, New York, 1996.
[20] L.A. Dombrovsky, A theoretical investigation of heat transfer by radiation under conditions of two-phase flow in a supersonic nozzle, High Temp. 34 (2) (1996) 255–262.
[21] L.A. Dombrovsky, Approximate methods for calculating radiation heat transfer in dispersed systems, Therm. Eng. 43 (3) (1996) 235–243.
[22] L.A. Dombrovsky, D. Baillis, Thermal Radiation in Disperse Systems: An Engineering Approach, Begell House, New York, 2010.
[23] V.V. Vinnikov, L.A. Dombrovsky, D.L. Reviznikov, A.V. Sposobin, Thermal radiation modeling in supersonic gas flow around a blunt body: effect of suspended particles, Therm. Proc. Eng. 4 (7) (2012) 312–318 (in Russian).
[24] L.A. Dombrovsky, D.L. Reviznikov, Radiative heat transfer modeling in supersonic gas flow with suspended particles to a blunt body, Heat Transfer 2014, in: Proc. 15th Int. Heat Transfer Conf., 10–15 August 2014, Kyoto, Japan, 2014, Paper 8214.
[25] L.A. Dombrovsky, Radiation of isothermal polydisperse layer, High Temp. 14 (4) (1976) 733–737.
[26] L.A. Dombrovsky, M.B. Ignatiev, An estimate of the temperature of semitransparent oxide particles in thermal spraying, Heat Transfer Eng. 24 (2) (2003) 60–68.
[27] O. Dufaud, M. Traoré, S. Perrin, S. Chazelet, D. Thomas, Experimental investigation and modeling of aluminum dusts explosion in the 20 L sphere, J. Loss Prev. Process. Ind. 23 (2) (2010) 226–236.
[28] P. Fauchais, G. Montavon, G. Bertrand, From powders to thermally sprayed coatings, J. Therm. Spray Technol. 19 (1–2) (2010) 56–80.
[29] D. Laredo, D.W. Netzer, The dominant effect of alumina on nearfield plume radiation, J. Quant. Spectrosc. Radiat. Transfer 50 (5) (1993) 511–530.
[30] G. Cai, D. Zhu, X. Zhang, Numerical simulation of the infrared radiative signatures of liquid and solid rocket plumes, Aerosp. Sci. Technol. 11 (6) (2007) 473–480.
[31] L.A. Dombrovsky, Large-cell model of radiation heat transfer in multiphase flows typical for fuel–coolant interaction, Int. J. Heat Mass Transfer 50 (17–18) (2007) 3401–3410.
[32] L.A. Dombrovsky, M.V. Davydov, P. Kudinov, Thermal radiation modeling in numerical simulation of melt–coolant interaction, Comput. Therm. Sci. 1 (1) (2009) 1–35.
[33] L.A. Dombrovsky, Thermal radiation modeling in multiphase flows of melt-coolant interaction, in: L. Cheng, D. Mewes (Eds.), Advances in Multiphase Flow and Heat Transfer, vol. 1, Bentham Science Publishing, 2009, pp. 114–157 (Chapter 4).
[34] D.L. Reviznikov, A.V. Sposobin, L.A. Dombrovsky, Radiative heat transfer from supersonic flow with suspended polydisperse particles to a blunt body: effect of collisions between particles, Comput. Therm. Sci. (2015). in press.
[35] D.S. Mikhatulin, D.L. Reviznikov, Modeling heat-erosion destruction of HAC elements during flight in a dusty atmosphere, Heat Transfer Res. 38 (2) (2007) 107–122.
[36] L.A. Dombrovsky, Evaluation of the error of the P_1 approximation in calculations of thermal radiation transfer in optically inhomogeneous media, High Temp. 35 (4) (1997) 676–679.
[37] V.M. Borisov, A.A. Ivankov, The P_1 and P_2 approximations of the spherical harmonic method as applied to radiative heat transfer computations with allowance for strong blowing from the surface of a vehicle moving in the Jovian atmosphere, Comput. Math. Math. Phys. 46 (9) (2006) 1611–1622.
[38] D.A. Andrienko, S.T. Surzhikov, P_1 approximation applied to the radiative heating of descent spacecraft, J. Spacecraft Rockets 49 (6) (2012) 1088–1098.
[39] L.A. Dombrovsky, W. Lipiński, A combined P_1 and Monte Carlo model for multi-dimensional radiative transfer problems in scattering media, Comput. Therm. Sci. 2 (6) (2010) 549–560.
[40] R.D. Cadle, Particles in the Atmosphere and Space, Reinhold, New York, 1966.
[41] C.L. Tien, S.C. Lee, Flame radiation, Prog. Energy Combust. Sci. 8 (1) (1982) 41–59.
[42] A.G. Blokh, Heat Transfer in Steam Boiler Furnaces, Hemisphere, New York, 1988.
[43] R. Viskanta, Radiative Transfer in Combustion Systems: Fundamentals and Applications, Begell House, New York, 2005.
[44] A. Harten, P.D. Lax, B. van Leer, On upstream differencing and Godunov-type schemes for hyperbolic conservation laws, Soc. Ind. Appl. Math. (SIAM) Rev. 25 (1) (1983) 35–61.
[45] M.E. Hayder, F.Q. Hu, M.Y. Hussaini, Towards perfectly absorbing boundary conditions for Euler equations, NASA CR-201689, Inst. Comput. Appl. Sci. Eng. (ICASE), Report No. 97–25, 1997.
[46] P.G. Saffman, The lift of small sphere in a slow shear flow, J. Fluid Mech. 22 (2) (1965) 385–400.
[47] L.A. Dombrovsky, E.P. Yukina, Critical conditions for inertial particle deposition from a gas flow near the stagnation point, High Temp. 21 (3) (1983) 402–408.
[48] L.A. Dombrovsky, Inertial deposition of particles from gas-disperse flow in the vicinity of stagnation point, High Temp. 24 (3) (1986) 429–434.
[49] D.L. Reviznikov, A.V. Sposobin, Numerical modeling of interaction of particles suspended in a supersonic flow with the blunt body surface, Math. Model. 19 (11) (2007) 101–111 (in Russian).
[50] D.L. Reviznikov, A.V. Sposobin, Calculations of supersonic flow about bodies in the case of suspended polydisperse particles, Trans. Moscow Aviat. Inst. 20 (3) (2013) 205–211 (in Russian).
[51] C.B. Henderson, Drag coefficients of spheres in continuum and rarefied flows, AIAA J. 14 (6) (1976) 707–708.
[52] B. Oesterlé, B.T. Dinh, Experiments on the lift of a spinning sphere in a range of intermediate Reynolds numbers, Exp. Fluids 25 (1) (1998) 16–22.
[53] S.I. Rubinow, J.B. Keller, The transverse force on a spinning sphere moving in viscous fluid, J. Fluid Mech. 11 (3) (1961) 447–459.
[54] S.C.R. Dennis, S.N. Singh, D.B. Ingham, The steady flow due to a rotating sphere at low and moderate Reynolds numbers, J. Fluid Mech. 101 (2) (1980) 257–279.
[55] T.W. Fox, C.W. Rackett, J.A. Nicholls, Shock wave ignition of magnesium powders, in: Proc. 11-th Int. Shock Tubes and Waves Symp., Seattle, 1978, pp. 262–268.
[56] A.N. Volkov, Yu.M. Tsirkunov, CFD/Monte Carlo simulation of collision-dominated gas-particle flows over bodies, in: Proc. of ASME Fluid Eng. Div. Summer Meeting, 14–18 July 2002, Montreal, Quebec, Canada, 2002, Paper 31222.
[57] V.V. Vinnikov, D.L. Reviznikov, A.V. Sposobin, Deterministic and statistical approaches to numerical modeling of a gas flow with suspended particles, Trans. Moscow Aviat. Inst. 17 (6) (2010) 13–19 (in Russian).
[58] J.R. Howell, R. Siegel, M.P. Mengüç, Thermal Radiation Heat Transfer, CRC Press, New York, 2010.
[59] M.F. Modest, Radiative Heat Transfer, third ed., Acad. Press, New York, 2013.
[60] J.J. Derby, S. Brandon, A.G. Salinger, The diffusion and P_1 approximations for modeling buoyant flow of an optically thick fluid, Int. J. Heat Mass Transfer 41 (11) (1998) 1405–1415.
[61] G. Li, M.F. Modest, A method to accelerate convergence and to preserve radiative energy balance in solving the P_1 equation by iterative methods, ASME J. Heat Transfer 124 (3) (2002) 580–582.
[62] D.A. Kontogeorgos, E.P. Keramida, M.A. Founti, Assessment of simplified thermal radiation models for engineering calculations in natural gas-fired furnace, Int. J. Heat Mass Transfer 50 (25–26) (2007) 5260–5268.
[63] L.C. Hartung, H.A. Hassan, Radiation transport around axisymmetric blunt body vehicles using a modified differential approximation, AIAA J. Thermophys. Heat Transfer 7 (2) (1993) 220–227.
[64] L.A. Dombrovsky, The use of transport approximation and diffusion-based models in radiative transfer calculations, Comput. Therm. Sci. 4 (4) (2012) 297–315.
[65] R.N. Edwards, R.P. Bobcôo, Radiant heat transfer from isothermal dispersion with isotropic scattering, ASME J. Heat Transfer 89 (4) (1967) 300–308.
[66] H.C. Van de Hulst, Light Scattering by Small Particles, Wiley, New York, 1957 (also Dover Publ., New York, 1981).
[67] C.F. Bohren, D.R. Huffman, Absorption and Scattering of Light by Small Particles, Wiley, New York, 1983.
[68] C.L. Tien, B.L. Drolen, Thermal radiation in particulate media with dependent and independent scattering, Annual Review of Numerical Fluid Mechanics and Heat Transfer, vol. 1, Hemisphere, New York, 1987, pp. 1–32.
[69] A.A. Kokhanovsky, Optics of Light Scattering Media: Problems and Solutions, third ed., Praxis, Chichester (UK), 2004.
[70] M.I. Mishchenko, L.D. Travis, A.A. Lacis, Multiple Scattering of Light by Particles: Radiative Transfer and Coherent Backscattering, Cambridge Univ. Press, New York, 2006.